ACS EARTH AND SPACE CHEMISTRY

http://pubs.acs.org/journal/aesccq

Article

Phosphorus Chemistry in Plant Ash: Examining the Variation across Plant Species and Compartments

Yudi Wu, Lois M. Pae, Chunhao Gu, and Rixiang Huang*

Cite This: *ACS Earth Space Chem.* 2023, 7, 2205−2213

Read Online

ACCESS | Metrics & More | Article Recommendations | Supporting Information

ABSTRACT: Natural terrestrial ecosystems are often phosphorus (P)-limited and rely heavily upon the internal cycling of P in plant litter. Fires thoroughly transform the aboveground P pools by turning litter (and living biomass) into ash and charcoal, changing the forms and fluxes of P entering soil. Therefore, it is important to understand the chemistry and availability of P in the burned residues to predict the impacts of fire on P cycling. This study characterizes the speciation and availability of P in fire ash produced from different plant species and compartments to explore P thermochemistry during biomass burning and geochemical behavior of fire ash. Great variations in P availability (measured by bicarbonate extractable P) were observed for ashes derived from compartments of a range of coniferous and deciduous trees, with labile P ranging from 9 to 78% of total P. Combining sequential extraction and P X-ray absorption near edge structure spectroscopy, we identified the main P species in ash, with apatite being the dominant P species (which contributes to the HCl-extractable P pool). A correlation between elemental stoichiometry and P availability indicates that relative abundances of the main P-complexing cations (i.e., calcium, potassium, and magnesium) affect P chemistry and mobility in ash, while the relationships depend upon plant species and compartments. Results from this study reveal how initial biomass composition (because of different physiological roles of macronutrients in plant compartments) and complete burning affect ash P chemistry and improve our understanding of the disturbance of vegetative fire to ecosystem characteristics and processes.

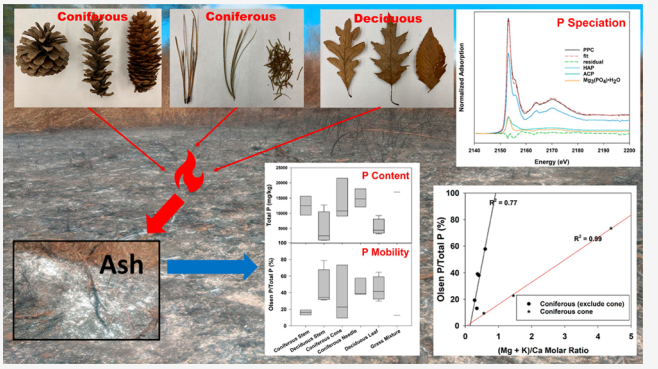

KEYWORDS: *vegetation fire, ash, phosphorus cycle, phosphorus speciation, XANES*

1. INTRODUCTION

Vegetation fires are a pervasive disturbance to many terrestrial ecosystems, because they result in not only immediate combustion of plant biomass and litter but also lasting impacts on the ecosystem structure and processes.[1,2] Vegetation fires burn 400−500 million hectares annually, which is equivalent to 4% of vegetated land surface on Earth.[3] Fires convert living plant, litter, and organic soil into ash and charcoal (being the complete and incomplete combustion products, respectively), extensively changing the aboveground pools and forms of carbon (C) and various nutrients.[4] Because of their enriched nutrient contents and changed physicochemical forms compared to plant biomass and litter, burn residues are important sources of C and nutrients to soils and can change soil chemical composition and properties.[5,6] Understanding the chemical forms and mobility of related elements is critical for evaluating the impacts of fire on elemental cycling in soils. Phosphorus (P) is often a limited nutrient in natural terrestrial ecosystems.[7] As pedogenesis continues and the ecosystem develops, soil P availability increasingly relies on internal P recycling (via litter decomposition) and external P inputs (mainly rock weathering and atmospheric deposition) become less important.[8,9] Therefore, it is important to evaluate the changes to aboveground P pools and forms by fire, which largely determine the mobility of P and its flux into soils.

Dependent upon the ecosystem composition and fire severity, the fuel sources (e.g., litter and living biomass from different plant species and compartments) and properties of burning products can be highly variable.[10−12] Chemical composition of these fuel sources and fire conditions, such as the temperature and duration, largely determine the production rate and properties of burned residues. Most P in plants and litter ends up in ash and charcoal after fires, because P volatilizes at a relatively high temperature (about 770 °C).[5] With regard to the speciation of P (i.e., molecular structure and

Received: May 26, 2023
Revised: October 3, 2023
Accepted: October 3, 2023
Published: October 22, 2023

complexation states), it has been relatively clear that P is mineralized and phosphate minerals are formed during biomass burning/combustion. For example, P extracted from charcoal and ash is mainly orthophosphate [confirmed by ^{31}P liquid nuclear magnetic resonance (NMR) spectroscopy],[13,14] and apatite is the main phosphate mineral identified [by X-ray diffraction (XRD)] in ash.[15] Studies also have revealed that the P mobility varies between burned residues (plant sources). For example, residues produced from litters of two different forests (Norway spruce and beech) have significantly different P mobilities.[16] Despite the progress in understanding the chemical forms and mobility of P in fire residues, variations in P chemical forms have not been quantitatively evaluated across plant species and compartments, and little is known about how P chemical forms affect ash P mobility. Because biomass chemical composition differs broadly between plant compartments and species, which contribute differentially to litter and fire fuels, it is necessary to evaluate the impacts of fuel composition on the P chemistry and mobility of burned residues.

The aim of this study is to characterize and correlate P speciation and availability of plant ashes and to determine the variation in ash P chemistry and impacts of initial biomass composition. We hypothesize that elemental stoichiometry (especially molar ratios between P and P-complexing metals) primarily controls P speciation in ash. Therefore, a diversity of biomass samples was selected, covering several widespread coniferous and deciduous plant species and litter-forming compartments and varying broadly in elemental stoichiometry. To obtain quantitative P speciation information and to explore P transformation during vegetation fire, complementary P speciation techniques, the Hedley extraction and P X-ray absorption near edge structure (XANES), are used. Availability of P (measured by bicarbonate extractable P) in ash is further correlated with stoichiometry of the main P-complexing metals in ash to explore the impacts of biomass composition. In this work, we focus only on ash, the complete combustion product, because ash and charcoal differ greatly in overall physicochemical properties and P chemistry. Ash is a completely inorganic matrix, and controls of P availability (solubility) are purely chemical (e.g., dissolution of phosphates or desorption of adsorbed phosphates), unlike charcoal that may be interfered with by other factors (P may be physically restrained in charcoal).

2. MATERIALS AND METHODS

2.1. Sampling. Plant compartments of *Pinus rigida* (pitch pine) and *Pinus strobus* (white pine) were collected from the Pine Bush Preserve, and *Picea abies* (Norway spruce) cone and needle were collected from the Five Rivers Environmental Education Center, both located in Albany, NY, U.S.A. Parts of deciduous trees, including *Quercus rubra* (red oak), *Quercus alba* (white oak), *Acer rubrum* (red maple), and *Fagus* (beech), were collected from a residential neighborhood in Albany, NY, U.S.A. All leaves (except spruce needle) are senesced leaves collected randomly from at least three different locations. Wood parts (bark, twig, and hardwood) were collected from living plants during tree cutting. The biomass was dried in an oven at 80 °C for at least 3 days until no weight change, before pulverizing by a single-speed blender (Hamilton Beach). Grass ash was prepared from a fresh prescribed fire at the Pine Bush Preserve (burn of mixed grasses in December of 2021), by further heating the prescribed fire residue in air at 550 °C until no weight change.

2.2. Ash Production. The pulverized biomass was placed in glass containers and heated in a benchtop furnace (Thermolyne, Thermos Scientific) in air. We recognized that thermal conditions can be highly variable during wildfires and can affect final ash composition and properties. Because our focus in this work is to compare P chemistry across a wide range of plant species and parts, we produced ash consistently at 550 °C for about 8−12 h (to ensure complete combustion of biomass), to avoid potential interference of the temperature effect.

2.3. Characterization of the General Physical and Chemical Properties. Elemental composition (C, H, N, and S) of biomasses was determined using a dry combustion method via a CHNS elemental analyzer (2400 Series II, PerkinElmer, Inc., Waltham, MA, U.S.A.). Approximately 1−10 mg of sample was used (combusted at 925 °C chamber), and the analysis was performed in triplicate. Analysis of the total contents of other major macronutrients in both biomass and ash, including K, Ca, Na, Mg, Mn, Al, Fe, and P, was provided by the Cornell Nutrient Analysis Laboratory. The elements were dissolved by a hot plate digestion method and determined by inductively coupled plasma optical emission spectrometry (ICP−OES) following United States Environmental Protection Agency (U.S. EPA) Method 6010-B. Specifically, a representative sample of up to 0.5 g (biomass) or 50 mg (ash) was digested in 5 mL of 60% nitric acid and 0.5 mL of hydroxide peroxide. The solid and solvent mixture was digested under heated conditions, and H_2O_2 was added twice to ensure complete digestion. After digestion, the sample was further diluted with deionized water prior to instrumental analysis. Composition data of raw biomass and ash can be found in Table 1 and Table S1 of the Supporting Information, respectively.

2.4. Characterization of Phosphorus Availability by Solution Extraction. *2.4.1. Measurement of Olsen P and Its Release Kinetics.* Soil P availability is commonly determined by bicarbonate extraction, and the extracted P is termed Olsen P.[17,18] The Olsen P content and its release kinetics were determined for ash samples. Approximately 100 mg of ash was added to 100 mL of 0.5 M $NaHCO_3$ solution in a 125 mL glass bottle. The bottle was capped and continuously agitated at 120 rpm and room temperature (20 °C). To determine the release kinetics, 3 mL of sample was withdrawn at specific time intervals (0.5, 1, 2, 3, 4, 8, 12, 24, 48, and 120 h) and filtered through a 0.45 μm (nylon) membrane. In a parallel set of bottles, samples were continuously agitated for 16 h, and the extracted P was determined as the Olsen P content of the ash. The phosphate content in the solution was analyzed using the ascorbic acid assay[19] on an ultraviolet−visible (UV−vis) spectrophotometer (UV-1900, Shimadzu, Japan). For each time point, the released P fraction (P_{Olsen}, %) was calculated using the following equation:

$$P_{Olsen} = \frac{C_x V}{C_p m} \quad (1)$$

where C_x (mg/L) is the P concentration in solution, V is the volume of $NaHCO_3$ solution (L), C_p is the total P concentration in ash (mg/g), and m is the mass of added ash (g).

https://doi.org/10.1021/acsearthspacechem.3c00145
ACS Earth Space Chem. 2023, 7, 2205−2213

Table 1. Elemental Compositions of Plant Compartments from Selected Coniferous and Deciduous Plants ($n \geq 3$ for Measurements with Standard Deviations)

plants	plant parts	label	ash content (%)	C (%)	H (%)	N (%)	S (%)	P (mg/kg)	K (mg/kg)	Ca (mg/kg)	Mg (mg/kg)	Mn (mg/kg)	Fe (mg/kg)	Zn (mg/kg)
pitch pine	cone	PPC	2.0 ± 0.3	51.0 ± 0.4	5.8 ± 0.1	0.3 ± 0.1	1.1 ± 0.1	186.0	196.5	1148.5	220.6	29.3	269.5	17.0
	needle	PPN	2.1 ± 0.1	53.5 ± 0.1	6.4 ± 0.1	0.4 ± 0.1	1.3 ± 0.2	392.5	624.1	4783.8	610.1	291.4	153.8	40.3
	twig	PPT	1.0 ± 0.4	54.3 ± 0.3	6.1 ± 0.1	0.6 ± 0.2	1.4 ± 0.1	267.0	210.1	2055.6	251.2	95.9	179.0	32.8
	bark	PPB	1.0 ± 0.1	55.7 ± 0.1	5.3 ± 0.1	0.1 ± 0.3	1.2 ± 0.1	135.0	209.8	1575.1	86.6	24.1	88.4	7.4
white pine	cone	WPC	1.6 ± 0.1	52.1 ± 0.1	6.1 ± 0.2	0.1 ± 0.1	1.2 ± 0.1	296.4	1786.6	2134.0	684.8	124.9	203.4	28.9
	needle	WPN	2.9 ± 0.1	54.4 ± 0.5	6.4 ± 0.1	0.3 ± 0.1	1.2 ± 0.1	340.1	491.7	4795.9	735.0	454.3	85.7	37.0
spruce	cone	SC	1.4 ± 0.1	53.2 ± 0.1	5.7 ± 0.1	0.5 ± 0.1	1.1 ± 0.1	514.2	3736.3	1187.1	625.7	57.7	140.8	24.9
	needle	SN	6.0 ± 0.3	51.1 ± 0.1	6.3 ± 0.1	1.1 ± 0.3	1.5 ± 0.1	1001.7	4794.3	9444.1	678.1	130.2	164.9	53.0
beech	leaf	BL	7.7 ± 0.2	49.2 ± 0.1	5.9 ± 0.1	0.7 ± 0.3	1.4 ± 0.1	373.4	622.2	10073.1	476.8	158.3	311.6	46.8
white oak	leaf	WOL	6.4 ± 0.1	49.7 ± 0.2	5.9 ± 0.1	0.9 ± 0.3	1.4 ± 0.1	364.7	685.3	13309.6	749.8	190.9	237.7	17.6
red oak	leaf	ROL	5.3 ± 0.3	51.1 ± 0.1	6.3 ± 0.1	0.9 ± 0.3	1.5 ± 0.2	684.8	1368.2	11213.9	1479.4	352.7	196.9	33.4
	wood	ROW	0.8 ± 0.1	49.0 ± 0.3	6.1 ± 0.1	0.4 ± 0.1	1.3 ± 0.1	230.1	1473.7	8731.5	306.4	21.4	35.4	1.9
	bark	ROB	9.3 ± 0.3	48.7 ± 0.2	5.8 ± 0.1	0.3 ± 0.2	1.3 ± 0.1	180.6	1224.4	37085.4	327.3	59.2	24.7	1.5
maple	leaf	RML	7.2 ± 0.6	52.4 ± 0.1	5.9 ± 0.1	1.0 ± 0.1	1.3 ± 0.1	510.0	1029.4	14612.6	1208.9	174.2	319.6	26.3
	wood	RMW	2.3 ± 0.4	50.1 ± 0.4	6.0 ± 0.1	0.2 ± 0.1	1.3 ± 0.1	163.3	1112.4	1870.3	245.0	44.4	187.8	9.1
	bark	RMB	9.7 ± 0.4	50.7 ± 0.6	5.7 ± 0.1	0.7 ± 0.1	1.2 ± 0.1	309.9	1686.8	13571.5	426.1	173.9	104.2	52.1

The temporal release data were fitted by the pseudo-first-order, pseudo-second-order, and simple Elovich equations, to interpret the P release pattern of ashes in the present study (Table S3 of the Supporting Information).[20] A simple Elovich equation $[q_t = 1/\beta \ln(\alpha\beta) + (1/\beta)\ln(t)]$ is an empirical expression of two or three simultaneous first-order reactions, which is commonly used when experimental data are inadequately described by a first-order kinetic equation.[21] In this equation, q_t is the released amount at time t and parameters α (% P h^{-1}) and β [(% P)$^{-1}$] are both constants, representing an initial release rate when $t \rightarrow 0$ and a release constant later governed by the exponential law, respectively.[22] A simple Elovich equation has been applied to desorption/release systems, such as zinc desorption from vertisols,[23] P release from Iranian calcareous soils,[24] and P release from plant and manure-based biochar.[20] Goodness of fitting was evaluated by the coefficient of determination (R^2) and the standard deviation.

2.4.2. Hedley Sequential Extraction. Sequential fractionation of P in ashes was conducted in triplicate, following the modified Hedley sequential extraction method.[25] Specifically, 50 mg of ash was added to a 50 mL polypropylene centrifuge tube and sequentially extracted using 30 mL of extraction solution. The sample tubes were continuously shaken at 120 rpm and room temperature. The ash was first extracted using deionized water, followed by 0.5 M $NaHCO_3$, 0.1 M NaOH, and 1 M HCl, each lasting 16 h. The P pools extracted are soluble P, exchangeable P, mineral-adsorbed P, and insoluble P minerals, respectively. At the end of each step, the tubes were centrifuged at 3750 rpm for 20 min to separate the liquid and solid. The solid residual left at the end of 1 M HCl extraction was digested by aqua regia (HCl/HNO_3 = 3:1). Concentrations of P in extracted solution from each step and in the final solid residual were determined using the ascorbic acid assay.[19]

2.5. Phosphorus K-Edge XANES Spectroscopy Analysis. Phosphorus K-edge XANES is a non-destructive technique that can provide specific chemical speciation, which complements sequential extraction and other speciation tools to provide accurate P speciation information for complex environmental samples. Phosphorus XANES data of ash samples were collected at the soft X-ray micro characterization beamline (SXRMB) at the Canadian Light Source (CLS, Saskatoon, Canada) and 8BM beamline (TES) at the National Synchrotron Light Source II (NSLS-II, Upton, NY, U.S.A.). The ash samples were fine powder and, thus, were directly spread on a P-free carbon tape (attached to a sample holder) for XANES spectra collection. The data were collected in fluorescence mode using a Si(111) double-crystal monochromator and a four-element Si(Li) drift detector. More details can be found in the study by Gu et al.[26] Because different calibration methods were used at the two beamlines ($AlPO_4$ at CLS and hydroxyapatite at NSLS-II), the hydroxyapatite spectrum was always collected during each beamtime and used for energy recalibration (its first derivative peak was set at 2152.6 eV).

Because of the relatively high P concentrations and large signal-to-noise ratios of the spectra, only two scans were collected for each sample. No difference between the two scans was observed, suggesting no radiation-induced changes to P speciation. The spectra were collected from 2113.50 to 2226.25 eV, with the following steps: 2 eV for 2113.5−2140.5 eV, 0.15 eV for 2140.5−2171.4 eV, and 0.75 eV for

https://doi.org/10.1021/acsearthspacechem.3c00145
ACS Earth Space Chem. 2023, 7, 2205−2213

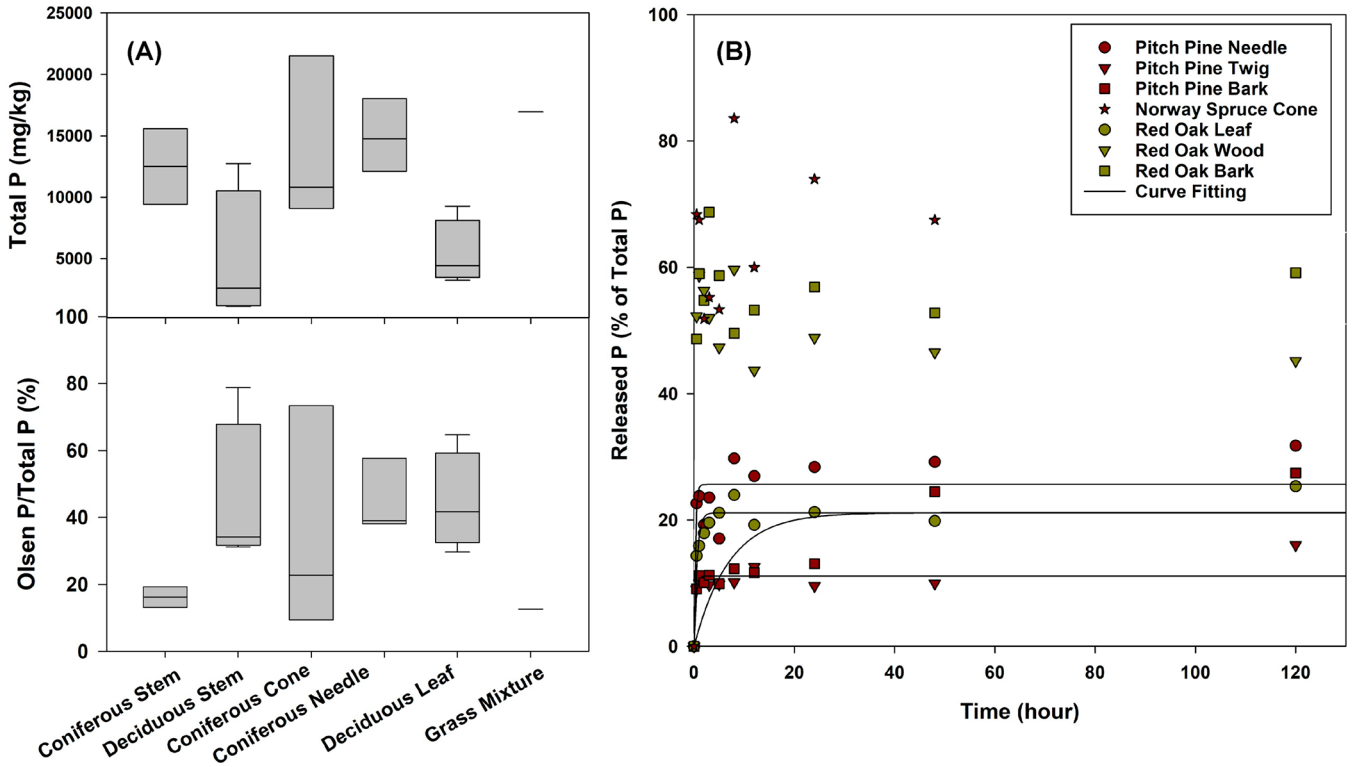

Figure 1. (A) Total P contents and Olsen P contents (percentage of total P) of ash produced from different compartments of deciduous and coniferous plants. Within each box, horizontal black lines indicate the median values. Boundaries of each box indicate 25th and 75th percentiles. Whiskers above and below the box are the 10th and 90th percentiles. (B) Temporal release of Olsen P for selected plant ashes and its fitting by the simple Elovich equation. Stems include wood, bark, and twigs of plants.

2171.4−2226.25 eV. The duplicate spectra were merged, backgroun-subtracted, and normalized before linear combination fitting (LCF). All analyses were performed using the Athena package.[27]

Phosphorus speciation in the samples was estimated using the LCF of the sample spectrum with those of reference compounds. We performed LCF on the processed XANES spectra at an energy range from 2142.5 to 2192.5 eV. Ca, K, and Mg are the most abundant metals with a metal/P molar ratio of >1 (Figure S1 of the Supporting Information) and, thus, are the most likely P-complexing cations. Therefore, a spectral library of the corresponding phosphate compounds was assembled. Principle component analysis (PCA) was first performed, which suggested that 99.5% variance can be explained by the first three components; thus, a maximum of three references was used in LCF. The appropriate reference compounds were selected by target transformation for LCF. The compounds include (1) amorphous calcium phosphate (ACP), (2) hydroxyapatite (HAP), (3) monopotassium phosphate, (4) trimagnesium phosphate octahydrate, and (5) dimagnesium phosphate trihydrate. Details of these reference compounds can be found in Table S2 of the Supporting Information, and their P K-edge XANES spectra are shown in Figure S3 of the Supporting Information. The goodness of fit was evaluated using the residual factor (R factor), and the fit with the smallest R factor was deemed the best fit.

3. RESULTS AND DISCUSSION

3.1. Chemical Compositions of Plant Biomass and Ash. Initial elemental composition of biomass largely determines the ultimate elemental composition of ash and may also play a role in controlling ash P speciation because P is completely mineralized in ash and the relative abundance of metals affects the potential of specific phosphate mineral formation. Elemental analysis shows that plant species and compartments differ broadly in elemental composition and stoichiometry, in terms of metal/P molar ratios (Table 1 and Figure S1 of the Supporting Information). Phosphorus contents in the dry biomass range from about 130 to 1000 mg/kg, and plant leaves have the highest P content (and N content) among all plant parts, regardless of tree species. Contents of other macronutrients in all types of biomass generally follow an order of Ca > K ≃ Mg > Na, while their concentration range differs greatly between plant species and parts. For example, the Ca concentration is relatively higher in deciduous trees than in coniferous trees (Table 1). Other metals, such as Na, Mn, Fe, and Zn, present at relatively low concentrations (1−400 mg/kg) in a way that needle/leaf or cone contained higher amounts than other tree parts (e.g., twigs, woods, or bark). As a result of the different concentration ranges, molar ratios of Ca, K, and Mg to P are much higher than 1, while ratios of Na, Mn, Fe, and Zn to P are relatively small, ranging from 0.01 to 1.6 (Figure S1 of the Supporting Information).

As the complete combustion product of biomass, ash consists of and retains most inorganic elements in biomass, because light elements, such as C, H, N, and S, are preferentially volatilized during combustion and the analyzed inorganic elements volatilize at temperatures much higher than 550 °C.[28] Overall, ash contents of deciduous tree parts (except for red oak wood at 0.8%) are relatively high, ranging from 2.3 to 9.7% compared to 1.0−2.9% for coniferous plants (except

https://doi.org/10.1021/acsearthspacechem.3c00145
ACS Earth Space Chem. 2023, 7, 2205−2213

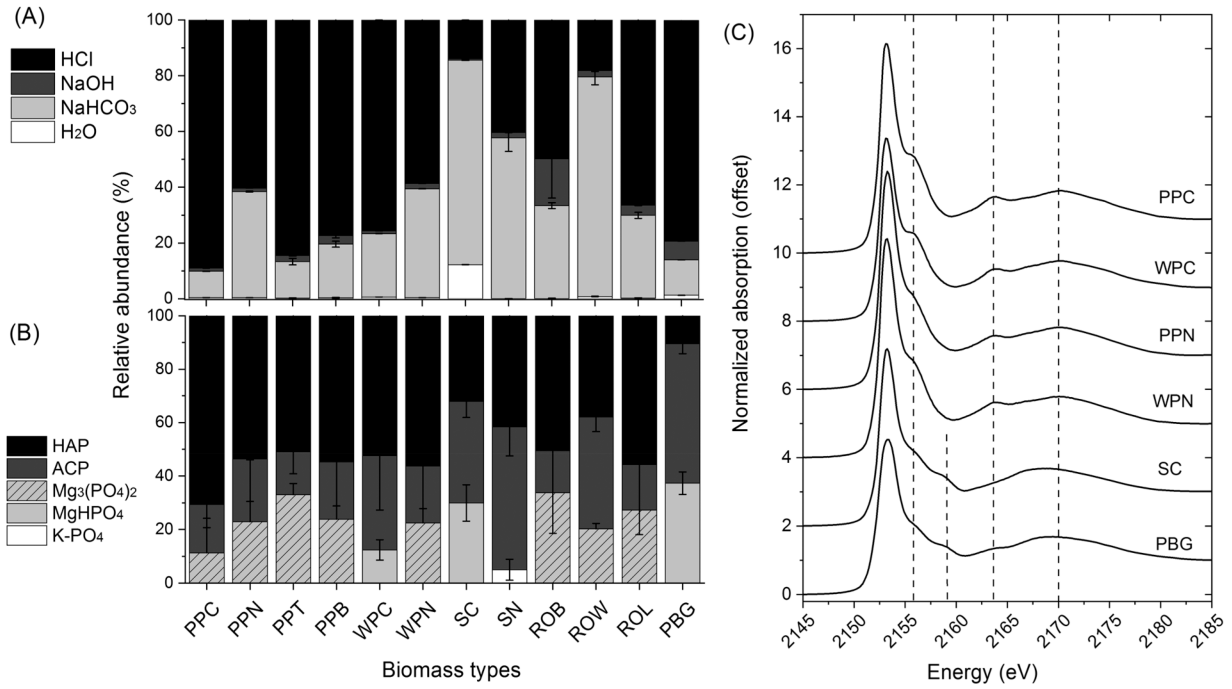

Figure 2. (A) Distribution of P in the Hedley fractionation pools. The error bar is the standard deviation of triplicate experimental results. (B) Relative abundance of different P species in ash samples as quantified by LCF of their P XANES spectra. The error bar is the uncertainty of fitting results. (C) Representative P K-edge XANES spectra and features of apatite signified by dashed lines (~2156, 2163, and 2170 eV). Two of the samples (SC and PBG) have an unidentified feature at 2159 eV.

for spruce needle at 6.0%) (Table 1). Ash retains similar elemental stoichiometries in biomass, with the preservation of the ash-forming elements in ash.

3.2. Phosphorus Availability and Speciation of Ash. *3.2.1. Phosphorus Availability Evaluated by Olsen P.* Bicarbonate ($NaHCO_3$) extract exchangeable P via an anion-exchange reaction, which is also known as Olsen P, is highly correlated with directly bioavailable P.[17] As shown by a study on wood ash soil application, the correlation between Olsen P and P uptake by plants is as high as 0.743 ($p < 0.001$).[29] Therefore, availability of P in ash was evaluated by the Olsen P content (percentage of total P), and great variation exists between ashes (Figure 1A and Figure S2 of the Supporting Information). The Olsen P content varies from 12 to 78%, and differences exist between plant parts and plant species. Cones of coniferous trees have a wide Olsen P content range of 16−73%. Plant leaves have a relatively small variation in the Olsen P contents (24−65%), and no significant difference between coniferous and deciduous trees were observed. Overall, coniferous tree stem and grass have relatively low Olsen P (<20%).

Release kinetics of Olsen P were measured for a range of ash samples (Figure 1B and Table S3 of the Supporting Information). Although the Olsen P contents vary broadly among ash samples, similar kinetic behaviors were found for all ashes (Figure 1B). Overall, Olsen P was rapidly released and stabilized within a few hours. The same kinetic behavior suggests the same chemical nature of Olsen P for all ash samples. The temporal release data were described by three kinetic models (i.e., first-order, second-order, and simple Elovich equations), and the simple Elovich equation has the best fitting result (Table S2 of the Supporting Information). Overall, the release coefficient β is similar (0.4−1.4), whereas α is different between ashes (Table S2 of the Supporting Information). The model failed to fit the data of a few ash samples, such as ashes of Norway spruce and red oak. These ashes immediately released all Olsen P within the first hour, indicating little dependency upon time. Overall, the simple Elovich equation reveals that α is the determining factor of P release because a larger α is associated with a larger Olsen P. The kinetic model indicates P release from ashes is a rapid process, possibly a result of rapid dissolution of soluble phosphate minerals or salts.

3.2.2. Phosphorus Speciation Evaluated by the Hedley Sequential Extraction and P XANES. To understand the chemical nature of P in fire ash, Hedley sequential extraction and P XANES analysis are complementarily used to obtain reliable and quantitative P speciation in ash. Sequential extraction shows that ash P was mainly partitioned in the $NaHCO_3$ and HCl extractable pools, while their relative abundances vary broadly between ashes of different plants and plant parts (Figure 2A). Overall, HCl extractable P ranges from 40 to 90% of total P in most ashes, except red oak wood (18%) and spruce cone (14%). Variation exists between plant parts, while no consistent pattern was observed for the two plant species (pitch pine and red oak).

All ash XANES spectra have features of Ca phosphates, although their intensity differs between samples (Figure 2 and Figure S3 of the Supporting Information). Fitting of the P XANES spectra showed that Ca and Mg phosphates are the main P species identified (Figure 2B and Table S4 of the Supporting Information). Calcium phosphates, including crystalline (HAP) and amorphous (ACP) Ca phosphates, are the dominant species in the characterized ashes, of which the sum accounts for 60−90% of total P. The other P species are Mg phosphate phases (Mg−P) and potassium phosphate (K−P). It is worth noting that SC and PBG have a feature at

https://doi.org/10.1021/acsearthspacechem.3c00145
ACS Earth Space Chem. 2023, 7, 2205−2213

~2159 eV that cannot be fitted, suggesting unrecognized species in these two samples (Figure 2C).

The predominance of Ca phosphates revealed by P XANES corresponds to the stoichiometric abundance of Ca (related to P and other metals) in ash (Figure S1 of the Supporting Information) and the abundance of HCl-extracted P pool. As shown in the correlation between XANES and sequential extraction results, the abundance of apatite correlates linearly (although deviates slightly from the 1:1 line) with the abundance of HCl-extracted P (Figure 3). This confirms that

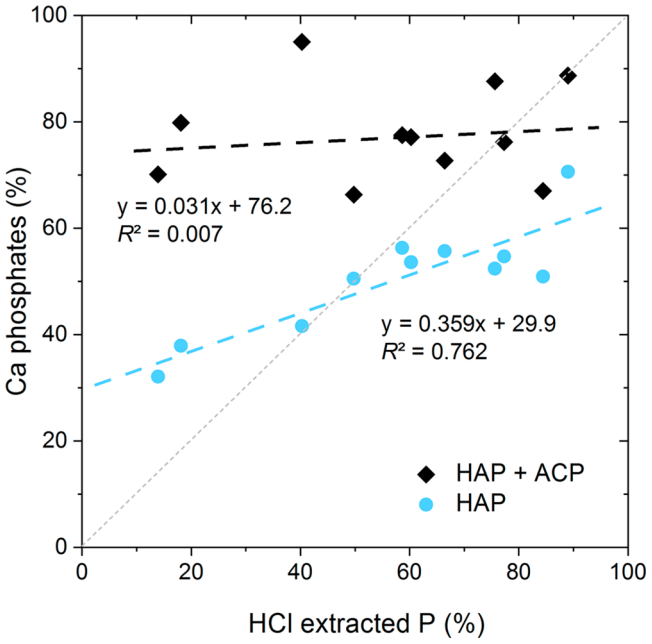

Figure 3. Correlation between HCl-extracted P and the abundances of HAP and HAP + ACP determined by the P XANES analysis. The gray short dashed line is the 1:1 line.

apatite identified by XANES corresponds to the HCl-extracted P pool. The sum of apatite and amorphous Ca phosphate does not correlate with HCl-extracted P (r^2 = 0.007) and is above the 1:1 line, suggesting that the identified amorphous Ca phosphate was extracted by H_2O and $NaHCO_3$ solution instead. The preferential extraction of non-apatite P species (including amorphous Ca phosphate) by $NaHCO_3$ solution is also reflected in the increasing abundance of apatite after $NaHCO_3$ extraction of the ashes of SC and SN (Figure S4 and Table S4 of the Supporting Information). For example, relative abundance of apatite was doubled after $NaHCO_3$ extraction that removed 60−70% P (Table S4 of the Supporting Information). The unrecognized species in SC ash was likely a soluble species, because the feature (2159 eV) disappeared after extraction.

3.3. Correlations between P Availability and Ash Elemental Composition. Composition and speciation data demonstrate that P chemistry is highly variable between ashes from plant species and plant parts and P exists mainly as Ca, Mg, and K phosphates. Therefore, a correlation was made between the P availability index and elemental stoichiometry, to reconcile the observed variation. Because Ca is the dominant metal and Ca phosphate is the main P species in ash, a correlation was first made between Ca phosphate abundance or Olsen P and Ca/P molar ratio, assuming that Ca phosphate abundance increases and Olsen P content (percentage of total P) decreases with increasing Ca/P ratios. Contradictory to our hypothesis, no clear relationships between them were observed when all ash samples (Figure 4A and Figure S5 of the Supporting Information) or categorized ash samples (panels B and C of Figure 4) were considered.

Because K and Mg are stoichiometrically abundant (K/P or Mg/P molar ratios are higher than 1) and compete for phosphate complexation in plant tissues, their abundance (relative to Ca) is expected to enhance P solubility (K and Mg phosphates are highly soluble). Therefore, a correlation may exist between Olsen P and (Mg + K)/Ca molar ratios. Similar to Ca/P ratios, no clear relationship was observed when the correlation was made for all ash samples (Figure 5A). However, a positive correlation appeared when the ash samples were divided and separately analyzed (panels B and C of Figure 5). Coniferous tree cones have a relatively wide range of (Mg + K)/Ca ratios, and their Olsen P increases linearly with the (Mg + K)/Ca ratios (R^2 = 0.99; Figure 5B). A positive linear correlation was also observed for other coniferous tree parts (i.e., needles and twig). In contrast, the relationship was not observed for deciduous tree parts, with a negative linear correlation even existing for the leaf ash (Figure 5C). A correlation was also made between Olsen P and Mg/P or K/P ratios, while all correlations were relatively poor (Figures S6 and S7 of the Supporting Information).

3.4. P Chemistry of Fire Ash: Impacts of Plant Physiology and Thermochemistry. Fire-burned residues are a significant P pool in fire-impacted ecosystems, and their inputs into soils strongly affect post-fire P cycling dynamics and soil nutrient states.[30] Although the heterogeneity of burned residues and dependence of residue properties upon initial biomass and fire conditions have long been recognized, the chemistry of P in fire ash and its relationship with P mobility are not well-understood.

This work aims to address these knowledge gaps, and the results greatly advance the current understanding in this field. First, by analyzing ash from a wide range of biomass sources, we were able to demonstrate that great variations in P chemistry exist between ashes of plant species and parts (Figure 1). Realizing such variation in evaluating the impact of fire on P cycling is necessary because ecosystem composition varies and fuels of a fire contributed differently by plant compartments. Second, with the combination of sequential extraction and P XANES analysis, this work first reveals quantitatively the speciation of P in ash. For example, with the advancement to previous studies that only qualitatively identify the presence of apatite in plant ash via XRD, we quantified and compared its relative abundance (and verified its equivalence to HCl-extracted P of the Hedley fraction) across a wide range of plant species and parts (Figure 2). Third, we also show that P speciation in ash does not necessarily reach an equilibrium state that correlates with elemental stoichiometry. With Ca phosphates being the most abundant P species in ash and controlling the (un)availability of P, it is tempting to assume that higher Ca/P ratios will lead to more Ca phosphate formation and less P availability, such as the use of the calcite content in explaining P availability.[16] By making a correlation between the Ca phosphate content or P availability and ash elemental stoichiometry [e.g., Ca/P and (Mg + K)/Ca molar ratios; Figure S5 of the Supporting Information and Figures 4 and 5], we reveal that the relative abundance of Ca phosphate

https://doi.org/10.1021/acsearthspacechem.3c00145
ACS Earth Space Chem. 2023, 7, 2205−2213

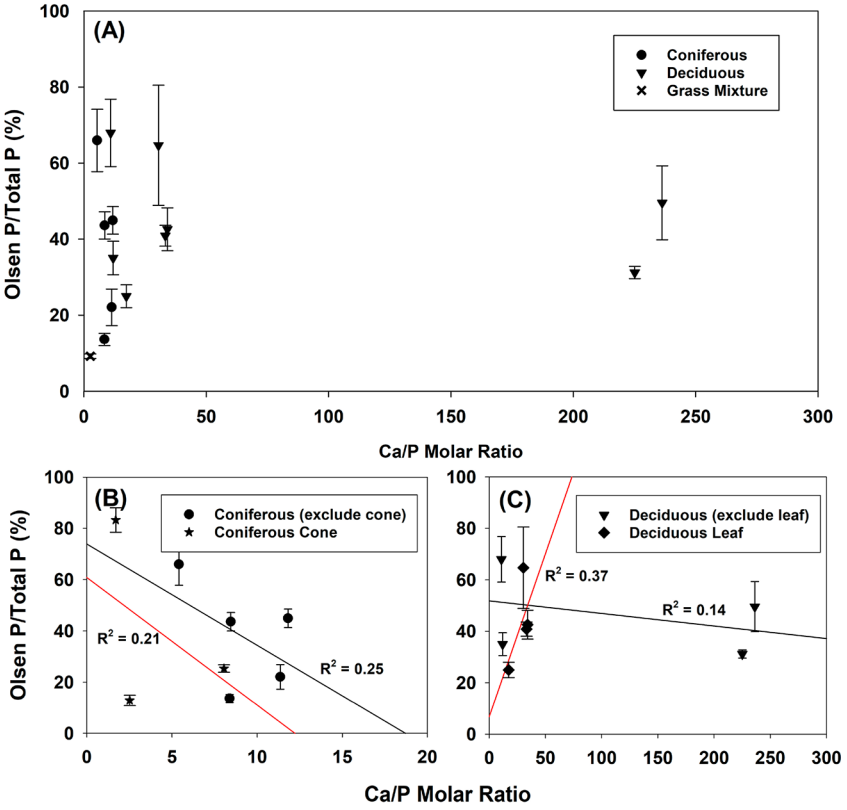

Figure 4. Olsen P/total P ratio versus Ca/P molar ratio for (A) all types of ashes, (B) coniferous ashes, and (C) deciduous ashes. Straight curves are linear regression fitting curves. Error bars are standard deviations of triplicate measurements of Olsen P.

or P availability is not proportional to elemental stoichiometry and binding affinity, at least not consistent across all ash types.

The great variation in ash P speciation and solubility (and inconsistent dependence upon elemental stoichiometry) reflects the compositional difference between plant species and different physiological roles of the analyzed macronutrients between plant parts. Phosphorus in biomass can exist in diverse molecular structures (i.e., orthophosphate, monoesters, diesters, and other organophosphorus) and complexation states (i.e., complexed by Ca or other metals), as structural, metabolic, or residual P.[31] Relative abundance of different P molecules and their complexation states are expected to vary between plant parts and growth stages because of the different roles of P between them. For example, plant seeds tend to store a great amount of P as phytate,[32] while leaves contain rich nucleic acids that are mineralized and resorbed during leaf senescence.[33,34] Complexation states of P molecules are unlikely to depend merely upon elemental stoichiometry because plant tissues are highly compartmented and concentrations of P and other macronutrients (as well as their interactions) are actively regulated. For example, a high abundance of Ca does not necessarily lead to more complexation of various P species by Ca in plant tissues, because plants regulate the concentrations and forms of Ca that are related to its role as a structural component or intracellular messenger (these functions do not directly involve the complexation with P).[35,36]

Combustion extensively transforms P speciation, while it remains unclear if it may differentially affect different biomass types in terms of P complexation and solubility. Although it is relatively clear that combustion induces organophosphorus mineralization and crystallization of phosphate minerals,[37] little is known about the changes to the metal complexation of phosphates. During complete combustion, organophosphorus is completely oxidized and phospho(di)ester bonds (P−O−R) in various organophosphates are broken and replaced by a cation. As a result, the difference in the organophosphorus content between biomass sources may affect the changes to P complexation induced by fires. At relatively high temperatures, P can be volatized and phosphate minerals can be molten, changing its chemical forms. If changes by fires are relatively small (e.g., the abundance of organophosphate is small), the complexation state of P in ash will depend primarily upon that in the initial plant biomass. To quantitatively understand these possible impacts of fires, future studies that can determine the relative abundances of organophosphorus and different metal complexes are needed.

4. CONCLUSION

Understanding the chemistry and mobility of nutrients in fire-burned residues has a range of important implications, considering the changes to ecosystem characteristics by fires and the significance of burned residues in post-fire nutrient cycling and nutrient stoichiometry of soils and plants. This study is the first attempt to examine detailed P speciation in ashes from a wide range of plant species and parts, and the results show that P chemistry in ash is heterogeneous and highly variable, depending upon the interactions between P and main P-complexing cations, like Ca, K, and Mg. The interactions are affected by the physiological functions of the macronutrients that vary between plant parts as well as the combustion process. The finding suggests a need to consider biomass stoichiometry and P chemistry in evaluating the immediate impacts of fires on aboveground nutrient pools. Our

https://doi.org/10.1021/acsearthspacechem.3c00145
ACS Earth Space Chem. 2023, 7, 2205−2213

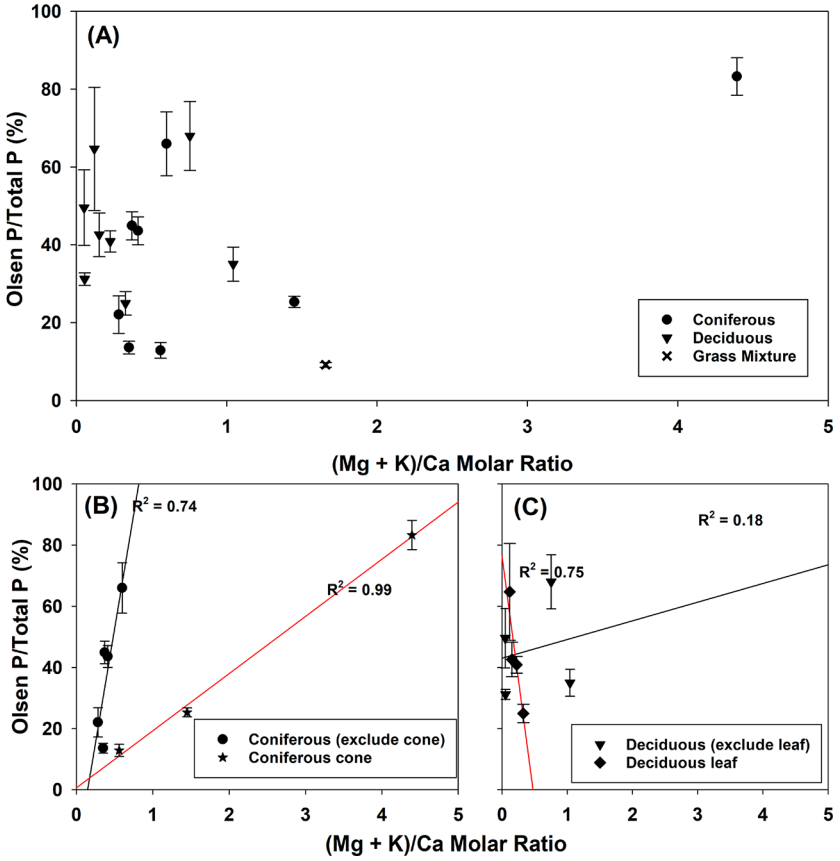

Figure 5. Olsen P/total P ratio versus (Mg + K)/Ca molar ratio for (A) all types of ashes, (B) coniferous ashes, and (C) deciduous ashes. Straight curves are the linear regression fitting curves. Error bars are standard deviations of triplicate measurements of Olsen P.

results also show that most ashes consist mainly of a relatively mobile P pool and a stable pool that constitutes crystalline Ca phosphates, suggesting that rapid dissolution of unstable phosphates and transport of soluble phosphates are likely to drive the initial cycling of ash P. At a later stage, transport and dissolution of Ca particulate phosphates may become more important. Such a mechanistic understanding is important for developing P cycling models and predicting the impacts of fire and ash deposition on soil nutrient states.

■ ASSOCIATED CONTENT

Supporting Information

The Supporting Information is available free of charge at https://pubs.acs.org/doi/10.1021/acsearthspacechem.3c00145.

Elemental composition of plant biomass and ash samples, model fitting results of Olsen P release kinetics, normalized P K-edge XANES spectra of reference compounds and ash samples and linear combination fitting results, and correlations between Olsen P and elemental molar ratios (PDF)

■ AUTHOR INFORMATION

Corresponding Author

Rixiang Huang − *Department of Environmental and Sustainable Engineering, University at Albany, Albany, New York 12222, United States;* orcid.org/0000-0001-8233-5223; Phone: 518-437-4977; Email: rhuang6@albany.edu

Authors

Yudi Wu − *Department of Environmental and Sustainable Engineering, University at Albany, Albany, New York 12222, United States*

Lois M. Pae − *Department of Environmental and Sustainable Engineering, University at Albany, Albany, New York 12222, United States*

Chunhao Gu − *Delaware Environmental Institute and Department of Plant and Soil Science, University of Delaware, Newark, Delaware 19716, United States*

Complete contact information is available at: https://pubs.acs.org/10.1021/acsearthspacechem.3c00145

Notes

The authors declare no competing financial interest.

■ ACKNOWLEDGMENTS

This work was supported by the National Science Foundation (Grant 2120547, 2021) and Startup Funds from University at Albany. The authors are grateful to the beamline scientists Mohsen Shakouri and Alisa Paterson at the Canadian Light Source and Yonghua Du and Seongmin Bak at the National Synchrotron Light Source II (NSLS-II) for help in collecting the P K-edge XANES spectra. A portion of the research described in this publication was performed at the Canadian Light Source, a national research facility of the University of Saskatchewan, which is supported by the Canada Foundation for Innovation (CFI), the Natural Sciences and Engineering Research Council (NSERC), the National Research Council (NRC), the Canadian Institutes of Health Research (CIHR),

the Government of Saskatchewan, and the University of Saskatchewan. Part of this research used beamlines 8-BM (TES) of the NSLS-II, U.S. Department of Energy (DOE) Office of Science User Facilities operated for the DOE Office of Science by Brookhaven National Laboratory (BNL) under Contract DE-SC0012704.

REFERENCES

(1) Pellegrini, A. F. A.; Harden, J.; Georgiou, K.; Hemes, K. S.; Malhotra, A.; Nolan, C. J.; Jackson, R. B. Fire effects on the persistence of soil organic matter and long-term carbon storage. *Nat. Geosci.* **2022**, *15* (1), 5−13.

(2) Bowd, E. J.; Banks, S. C.; Strong, C. L.; Lindenmayer, D. B. Long-term impacts of wildfire and logging on forest soils. *Nat. Geosci.* **2019**, *12* (2), 113−118.

(3) Bowman, D. M. J. S.; Kolden, C. A.; Abatzoglou, J. T.; Johnston, F. H.; van der Werf, G. R.; Flannigan, M. Vegetation fires in the Anthropocene. *Nat. Rev. Earth Environ.* **2020**, *1* (10), 500−515.

(4) Kauffman, J. B.; Cummings, D. L.; Ward, D. E. Relationships of Fire, Biomass and Nutrient Dynamics Along a Vegetation Gradient in the Brazilian Cerrado. *J. Ecol* **1994**, *82* (3), 519−531.

(5) Bodí, M. B.; Martin, D. A.; Balfour, V. N.; Santín, C.; Doerr, S. H.; Pereira, P.; Cerdà, A.; Mataix-Solera, J. Wildland fire ash: Production, composition and eco-hydro-geomorphic effects. *Earth Sci. Rev.* **2014**, *130*, 103−127.

(6) Caon, L.; Vallejo, V. R.; Ritsema, C. J.; Geissen, V. Effects of wildfire on soil nutrients in Mediterranean ecosystems. *Earth Sci. Rev.* **2014**, *139*, 47−58.

(7) Hou, E. Q.; Luo, Y. Q.; Kuang, Y. W.; Chen, C. R.; Lu, X. K.; Jiang, L. F.; Luo, X. Z.; Wen, D. Z. Global meta-analysis shows pervasive phosphorus limitation of aboveground plant production in natural terrestrial ecosystems. *Nat. Commun.* **2020**, *11* (1), 637.

(8) Walker, T. W.; Syers, J. K. The fate of phosphorus during pedogenesis. *Geoderma* **1976**, *15* (1), 1−19.

(9) Sohrt, J.; Uhlig, D.; Kaiser, K.; von Blanckenburg, F.; Siemens, J.; Seeger, S.; Frick, D. A.; Krüger, J.; Lang, F.; Weiler, M. Phosphorus Fluxes in a Temperate Forested Watershed: Canopy Leaching, Runoff Sources, and In-Stream Transformation. *Front. For. Glob. Change* **2019**, *2*, 85.

(10) Murphy, B. P.; Prior, L. D.; Cochrane, M. A.; Williamson, G. J.; Bowman, D. M. J. S. Biomass consumption by surface fires across Earth's most fire prone continent. *Global Change Biol.* **2019**, *25* (1), 254−268.

(11) Walker, X. J.; Baltzer, J. L.; Cumming, S. G.; Day, N. J.; Johnstone, J. F.; Rogers, B. M.; Solvik, K.; Turetsky, M. R.; Mack, M. C. Soil organic layer combustion in boreal black spruce and jack pine stands of the Northwest Territories, Canada. *Int. J. Wildland Fire* **2018**, *27* (2), 125−134.

(12) Hudak, A. T.; Ottmar, R. D.; Vihnanek, R. E.; Brewer, N. W.; Smith, A. M. S.; Morgan, P. The relationship of post-fire white ash cover to surface fuel consumption. *Int. J. Wildland Fire* **2013**, *22* (6), 780−785.

(13) Gray, D. M.; Dighton, J. Mineralization of forest litter nutrients by heat and combustion. *Soil Biol. Biochem.* **2006**, *38* (6), 1469−1477.

(14) García-Oliva, F.; Merino, A.; Fonturbel, M. T.; Omil, B.; Fernández, C.; Vega, J. A. Severe wildfire hinders renewal of soil P pools by thermal mineralization of organic P in forest soil: Analysis by sequential extraction and ^{31}P NMR spectroscopy. *Geoderma* **2018**, *309*, 32−40.

(15) Yusiharni, E.; Gilkes, R. Minerals in the ash of Australian native plants. *Geoderma* **2012**, *189*−*190*, 369−380.

(16) Schaller, J.; Tischer, A.; Struyf, E.; Bremer, M.; Belmonte, D. U.; Potthast, K. Fire enhances phosphorus availability in topsoils depending on binding properties. *Ecology* **2015**, *96* (6), 1598−1606.

(17) Olsen, S. R. *Estimation of Available Phosphorus in Soils by Extraction with Sodium Bicarbonate*; U.S. Department of Agriculture: Washington, D.C., 1954.

(18) Curtin, D.; Syers, J. K. Lime-Induced Changes in Indices of Soil Phosphate Availability. *Soil Sci. Soc. Am. J.* **2001**, *65* (1), 147−152.

(19) Murphy, J.; Riley, J. P. A modified single solution method for the determination of phosphate in natural waters. *Anal. Chim. Acta* **1962**, *27*, 31−36.

(20) Sun, K.; Qiu, M.; Han, L.; Jin, J.; Wang, Z.; Pan, Z.; Xing, B. Speciation of phosphorus in plant- and manure-derived biochars and its dissolution under various aqueous conditions. *Sci. Total Environ.* **2018**, *634*, 1300−1307.

(21) Chien, S. H.; Clayton, W. R. Application of Elovich Equation to the Kinetics of Phosphate Release and Sorption in Soils. *Soil Sci. Soc. Am. J.* **1980**, *44* (2), 265−268.

(22) Chien, S. H.; Clayton, W. R. Application of Elovich Equation to the Kinetics of Phosphate Release and Sorption in Soils. *Soil Sci. Soc. Am. J.* **1980**, *44* (2), 265−268.

(23) Dang, Y. P.; Dalal, R. C.; Edwards, D. G.; Tiller, K. G. Kinetics of Zinc Desorption from Vertisols. *Soil Sci. Soc. Am. J.* **1994**, *58* (5), 1392−1399.

(24) Shariatmadari, H.; Shirvani, M.; Jafari, A. Phosphorus release kinetics and availability in calcareous soils of selected arid and semiarid toposequences. *Geoderma* **2006**, *132* (3), 261−272.

(25) Hedley, M. J.; Stewart, J. W. B.; Chauhan, B. S. Changes in Inorganic and Organic Soil Phosphorus Fractions Induced by Cultivation Practices and by Laboratory Incubations. *Soil Sci. Soc. Am. J.* **1982**, *46* (5), 970−976.

(26) Gu, C.; Dam, T.; Hart, S. C.; Turner, B. L.; Chadwick, O. A.; Berhe, A. A.; Hu, Y.; Zhu, M. Quantifying uncertainties in sequential chemical extraction of soil phosphorus using XANES spectroscopy. *Environ. Sci. Technol.* **2020**, *54* (4), 2257−2267.

(27) Ravel, B.; Newville, M. ATHENA, ARTEMIS, HEPHAESTUS: Data analysis for X-ray absorption spectroscopy using IFEFFIT. *J. Synchrotron Radiat.* **2005**, *12* (4), 537−541.

(28) Boström, D.; Skoglund, N.; Grimm, A.; Boman, C.; Öhman, M.; Broström, M.; Backman, R. Ash Transformation Chemistry during Combustion of Biomass. *Energy Fuels* **2012**, *26* (1), 85−93.

(29) Erich, M. S. Agronomic Effectiveness of Wood Ash as a Source of Phosphorus and Potassium. *J. Environ. Qual.* **1991**, *20* (3), 576−581.

(30) Butler, O. M.; Elser, J. J.; Lewis, T.; Mackey, B.; Chen, C. R. The phosphorus-rich signature of fire in the soil-plant system: A global meta-analysis. *Ecol Lett.* **2018**, *21* (3), 335−344.

(31) Hidaka, A.; Kitayama, K. Allocation of foliar phosphorus fractions and leaf traits of tropical tree species in response to decreased soil phosphorus availability on Mount Kinabalu, Borneo. *J. Ecol* **2011**, *99* (3), 849−857.

(32) Lott, J. N. A.; Ockenden, I.; Raboy, V.; Batten, G. D. Phytic acid and phosphorus in crop seeds and fruits: A global estimate. *Seed Sci. Res.* **2000**, *10* (1), 11−33.

(33) Smith, A. P.; Fontenot, E. B.; Zahraeifard, S.; DiTusa, S. F. Molecular Components That Drive Phosphorus-Remobilisation during Leaf Senescence. In *Annual Plant Reviews*; Plaxton, W. C., Lambers, H., Eds.; John Wiley & Sons: Hoboken, NJ, 2015; Phosphorus Metabolism in Plants, Vol. *48*, Chapter 6, pp 159−186, DOI: 10.1002/9781118958841.ch6.

(34) Fries, N. Variations in the content of phosphorus, nucleic acids and adenine in the leaves of some deciduous trees during the autumn. *Plant Soil* **1952**, *4* (1), 29−42.

(35) Thor, K. Calcium—Nutrient and Messenger. *Front. Plant Sci.* **2019**, *10*, 440.

(36) White, P. J.; Broadley, M. R. Calcium in plants. *Ann. Bot.* **2003**, *92* (4), 487−511.

(37) Huang, R. X.; Fang, C.; Lu, X. W.; Jiang, R. F.; Tang, Y. Z. Transformation of Phosphorus during (Hydro)thermal Treatments of Solid Biowastes: Reaction Mechanisms and Implications for P Reclamation and Recycling. *Environ. Sci. Technol.* **2017**, *51* (18), 10284−10298.